Spectrochimica Acta Part B: Atomic Spectroscopy 190 (2022) 106391

Contents lists available at ScienceDirect

Spectrochimica Acta Part B: Atomic Spectroscopy

journal homepage: www.elsevier.com/locate/sab

Field deployment of a man-portable stand-off laser-induced breakdown spectrometer: A preliminary report on the expedition to the Cumbre Vieja volcano (La Palma, Spain, 2021)

Santiago Palanco [a,*], Raúl Pérez-López [b], Inés Galindo-Jiménez [b], Alberto Bernal [a], Sergio Aranda [a], María Cruz López-Escalante [a], Dietmar Leinen [a], Jose F. Mediato [b], Julio López-Gutiérrez [b], José R. Ramos-Barrado [a]

[a] Universidad de Málaga, Andalucía Tech, Departamento de Física Aplicada I, Campus de Teatinos, s/n, Málaga 29071, Spain
[b] Consejo Superior de Investigaciones Científicas, Instituto Geológico y Minero de España Departamento de Riesgos Geológicos y Cambio Climático, C/ Ríos Rosas 23, Madrid 28003, Spain

ARTICLE INFO

Keywords:
LIBS
Laser-induced breakdown spectroscopy
Stand-off
Remote
Man-portable
Volcanic eruption
Lava

ABSTRACT

This paper reports on the expedition to the Cumbre Vieja volcano (Canary Islands, Spain) in November 2021 to assess stand-off laser-induced breakdown spectroscopy for real-time measurements of the lava streams from a safe point. The paper provides insight on the analytical approach to the problem, the rationale of the instrument design and construction carried out in three weeks, the experience with the new-born instrument at the volcano and the preliminary results. Despite the subtle spectral differences among the samples and the signal variability induced by the strong wind gusts at site, a statistical approach to data processing such as PCA, made possible to extract sufficient information and provide a robust classification tool.

1. Introduction

On September 19th, 2021, the last volcano of La Palma (Canary Islands, Spain) emerged in the surroundings of the Cumbre Vieja Natural Park. The eruption broke a 50-year truce and it kept active until December 13th, 2021. Volcanic eruptions of basaltic magma show complex dynamics which determine the emergency response in the case of an urban eruption like this. The first stage of an eruption is the magma chamber emplacement, normally between 10 and 11 km deep for the volcanism of the Canary Islands [1]. At this stage, the time of magma storage is relevant to determine the mineral fraction stratigraphy, depending on the temperature and pressure of the magma chamber. When the eruption starts, the first erupted material is the upper part of the magmatic chamber, which determines the mineral composition of the lava, tephra, and ash. As the eruption and magma plumbing evolve, geochemical composition of the lava varies [2–4], and hence, it is possible to estimate the composition of the remaining magma chamber and the new conditions of temperature and pressure. In the case of the La Palma eruption, the first stage of similar historic basaltic volcanism is poor in olivine content, with amphibole, and clinopyroxene into a vitreous melange. Since the magma chamber is emptied at the final stages, there is an increase in olivine content and the basaltic lava is enriched in aluminium and plagioclase [5].

Geochemical and mineralogical composition is usually determined with laboratory analytical techniques days after the samples are collected and therefore loses its usefulness as an emergency tool to determine the stage of the eruption. The advantage to knowing the geochemical composition of lavas in real-time is the possibility to detect when the magma chamber has evolved. In situ determination of the geochemical composition provides an instant classification of lavas through graphs like total alkali vs silica diagrams (TAS) and rare earth elements (REE) of the primitive mantle [6]. Furthermore, reactivation by dike-feeding the magma chamber from the primary molten can be determined as well, allowing to interpret new stages and eruption rates. In summary, real-time determination of lava composition can show the evolution of the magma chamber and the eruption dynamics, allowing the estimation of the magma chamber's recharge.

Laser-induced breakdown spectroscopy (LIBS) is an analytical atomic emission spectroscopy technique which uses a high-peak-power laser pulse to induce a plasma on the sample surface. The light emitted

* Corresponding author.
E-mail address: spalanco@uma.es (S. Palanco).

https://doi.org/10.1016/j.sab.2022.106391
Received 4 January 2022; Received in revised form 24 February 2022; Accepted 24 February 2022
Available online 28 February 2022

by the plasma contains information on the sample components and their respective concentrations which can be revealed in real-time through its spectrochemical analysis. Furthermore, since LIBS is an all-optical technique, it can be implemented into configurations which allow remote analysis [7,8 and refs. therein]. But out of those instruments oriented to field analysis only a few are light and compact enough to be considered truly fieldable instruments [9–11].

Having recently developed a drone-borne compact LIBS instrument [12,13], it was considered for helping to minimize manual sampling of the lava streams while allowing for a more extensive sampling. The logical approach was to adapt the analytical method for lava samples and then fully test the instrument at the volcano. However, during the first weeks of the eruption a number of drones had crashed while at very-low level flight due to: (i) the high temperature and lower lift caused by the lava field, (ii) the double effect of the abrasive and magnetic volcanic ashes in drone rotors, and (iii) the lava magnetism seemingly affecting the inertial measurement units of the drones [14].

Thus, the decision was made to develop a man-portable stand-off LIBS instrument which could work at a minimum of 20 m from the lava streams and to assess how LIBS could fare in such harsh conditions within three weeks. The various prediction models converged in that the energy stored in the volcanic system could maintain the eruption for such timeframe. In addition, the emergency caused by the eruption affected logistics which, together with bureaucracy would prevent lava samples to be sent to the laboratory in time. In consequence, the instrument could only be tested with surrogate samples prior to departure.

Although at a first glance this might seem a somewhat risky approach, it must be understood in the context of a unique experimental endeavour. Formerly, the exceptionality of the circumstances justified other unusual tests even with no previous knowledge of the samples [15]. In the present case, the starting point was a better one as LIBS has been extensively used in the past for soil analysis both in the laboratory and in the field [16–21] and volcanic samples have been recently targeted with success in the laboratory [22–24]. In addition, LIBS has been assessed for the characterization of steel and its processing slags at high temperature [25–27], even in a liquid state [28]. However, to the best of our knowledge, no attempt has been made to measure the composition of lava streams in the field during an eruption. The aim of this paper is to report on the expedition to the Cumbre Vieja volcano eruption, providing insight into the analytical approach to the problem, the rationale of the instrument design and construction, the experience with an instrument in the hostile conditions at the volcano and the preliminary results and conclusions.

2. Analytical method and instrumentation

2.1. Information on lava samples

In the absence of lava samples at the laboratory for preparation of LIBS, the alternative was to gather as much information as possible to prepare suitable surrogates. The lava erupted at La Palma is mainly composed by a trachybasalt rock emitted as ’a’ā and pahoehoe lava types. Concerning the interaction with the laser beam, the lava is a matte black in colour, it presents an irregular surface topography, often with signs of bubbling or deep grooves. Thus, although it may have brittle surface areas, the bulk is tough. Extracting a lava sample is a heavy task even using tools such as a mountaineering axe. The composition interval measured on several samples of the current eruption with XRF is detailed in Table 1 and is in good agreement with the geochemical analysis from historic eruptions in the island -San Juan 1949, 1 km away from Cumbre Vieja, and Teneguía 1971 [29].

Basing on Table 1, pressed pellets of various salts were prepared along with a set of pure metal foils and chips for spectral reference and a tentative list of 78 spectral lines (247–780 nm) was elaborated basing in our previous experience with steels, steelmaking slags and suggestions from personnel of the Atomic Spectrometry Unit at the central facility for research support (SCAI-UMA) of the University of Málaga. The list served a double purpose: before the expedition it helped to select a spectrometer and a spectral window with the maximum number of most probably useable lines and thus, to be able to maximize the time at the field. During the expedition and afterwards, it helped with the identification of the lines of interest and spectral interferences. However, a definitive selection of the useful spectral lines (Table 2) was not made until spectra of actual lava samples were eventually acquired. In the meantime, it was assumed that the high sample content in Ti, Fe and Cr and the line-rich emission of these elements would interfere with the

Table 1
Concentration intervals for the elements of interest in lava samples.

Element	Concentration (% *w*/w)	
	Min	Max
Si	10	17
Fe	10	11
Ca	5.7	7.3
Al	3.7	6.7
Mg	0.8	3
Ti	1.9	2
K	0.9	1.8
Mn	0.1	0.15
Sr	0.1	0.12
	Concentration (ppm)	
Ba		<1000
Cu		<1000
V		<500
Zr		<500
Cr		<350
Sb		<250
Ce		<250
Zn		<250
La		<250
Nb		<150
Pb		<150
Ni		<100
Nd		<100
Y		<100
Sn		<100
Rb		<100
Cd		<100
Th		<100
Mo		<100

Table 2
List of spectral lines used for the study of lava samples. Ti, Fe, Mn: spectral interferences.

Wavelength (nm)	Element species	Comment
285.213	Mg(I)	
288.158	Si(I)	
298.357	Fe(I)	
302.064	Fe(I)	
308.215	Al(I)	Ti
309.271	Al(I)	
309.284	Al(I)	
315.887	Ca(II)	
317.933	Ca(II)	
334.941	Ti(II)	Mn
336.121	Ti(II)	Mn
337.279	Ti(II)	
341.476	Ni(I)	Fe, Ti
344.637	K(I)	weak
344.738	K(I)	
350.111	Ba(I)	
351.505	Ni(I)	Fe, Ti
353.212	Mn(I)	Fe, Ti
354.800	Mn(I)	Fe, Ti
357.009	Fe(I)	Mn
358.119	Fe(I)	Mn
359.346	Cr(I)	Fe, Ti

much scarcer and weaker emission of the minor elements. The problem would require either selecting the 280–360 nm window with a good resolution (<0.1 nm FWHM) plus the 402–457 nm window with a lower resolution <0.15 nm FWHM -and yet some elements such as Na might get discarded- or covering both windows with a lower resolution (~0.25 nm FWHM) and then, intensive post processing work would be required to try to deconvolute the spectral interferences (Fig. S1).

Regarding calibration for quantitative analysis, it was decided to use actual lava which would be sampled trying to maximize the composition range. To this end, the sampling is being spread in time and among the various centres of lava emission. Then, all samples will be characterized using ICP-MS at SCAI-UMA. Since the composition of the lava emitted varies throughout the eruption time, the spread of concentrations for the elements of interest should increase and thus, the extraction of samples from the various emission centres and streams will provide a set of samples with a maximized interval of compositions.

2.2. Rationale of instrument design and construction

Man-portability has strong implications on the instrument design as it conditions the size, weight, modularity and fragility for travel or transport in the field. Two main alternate instrument concepts (C1 and C2) were initially devised. According to Fig. 1, configuration C1 is designed to be transported and operated from a car boot. It is based on a Quantel Brilliant B laser (850 mJ, 6 ns, 10 Hz at 1064 nm) with a 0.5-mrad beam divergence. In our experience, a beam of such characteristics can produce plasmas of analytical quality at ~100 m when focused with optics ~100 mm in diameter. The downside of this configuration is the bulky laser power supply and cooling unit and hence, the need for operating from a car boot or not far from it. Configuration C2, instead, uses a Quantel Viron laser (25 mJ, 5 ns, 20 Hz at 532 nm) with a beam divergence of 1.5 mrad. There is no particular reason to use the second harmonic -it is built in the laser unit available. If anything, the second harmonic is safer to operate than the fundamental since it is visible. The power supply is integrated with the laser head in this unit whose weight is below 3 kg. From a previous experience working at 10 m, we presumed that there was room to stretch that distance to 50 m. This would provide a safe distance to the streams and a lighter, more modular instrument which can be transported by the personnel at site and quicky assembled at the point of analysis.

By October 17th, almost a month into the eruption, the topography of the terrain and that of the lava streams had undergone a profound transformation with the build-up of tall, thick dam-like walls which prevented a direct line of sight to the flows from the remaining tracks. In consequence, configuration C2 was chosen over C1, basing on portability as it could be an advantage to gain a watchtower to the lava.

Two equivalent optical systems were designed for the laser emitter side of C2 (Fig. 2) and all the components for both designs were ordered so that a backup system was available in the case of a stock shortage or a delay in the delivery of a component. The two optical models were nearly diffraction limited in the range between 25 m and 50 m from the instrument -over 96% of the laser energy was contained within the airy disk- and each one comprised three spherical singlets (Table 3). The length of the optical path was increased to achieve a large expansion ratio while preventing optical aberration from significantly impacting the performance or the dimensions and weight balance of the assembly. On the mechanical side, the emitter is designed around a back-thinned aluminium plate which holds the laser and batteries, two folding mirrors and either of both optical configurations detailed in Table 3. The three lenses are held by a carbon-fibre tube mount which allowed fine focus adjustment. Overall, the length of the emitter unit is comparable to that of the receiver.

Regarding the collection of the plasma light, a UV-coated aluminium mirror of the required characteristics (150–200 mm diameter, 350–750 mm focal length) could not be found in a short timeframe. Instead, the UV performance of three commercially available Newtonian telescopes was evaluated. Naming the brand and model of the three units would be misleading as it was found that a one-year separation in two batches of the same model offered substantially different throughputs. The unit finally selected (150 mm in diameter, F/5) has a reflectance between 75% at 270 nm and 90% at 589 nm.

Despite not covering the entire spectral region and lacking the required resolution, the best spectrometer option available in the laboratory at that time was a combination of an Andor Shamrock 163 spectrograph and a DH740 iCCD detector basing on sensitivity and weight. The specifications are detailed in Table 4. As a backup unit, a customized compact USB spectrometer (S1 in Table 4) was selected. The acquisition delay was set at 800 ns from the laser output once the distance-dependent delay is subtracted and the acquisition gate was 2 μs. Given the modular design of the instrument, a UV fibre optic cable (core diameter 100 μm, length 2 m) was used even if a better light throughput to the spectrograph would be achieved by directly coupling

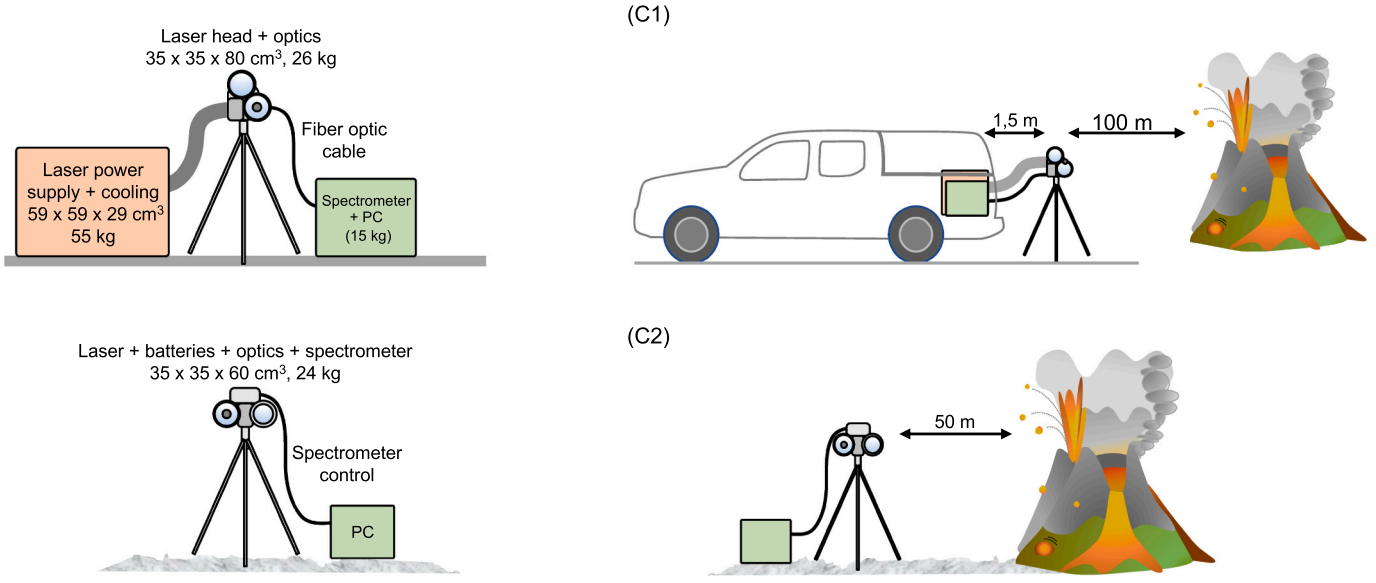

Fig. 1. Illustration of the two instrumental concepts considered for the expedition. C1 is a transportable 100-m Stand-off LIBS instrument which must be operated from or close to a vehicle. C2 is a modular man-portable (two person) instrument which can be assembled on site to perform Stand-off LIBS up to ~50 m.

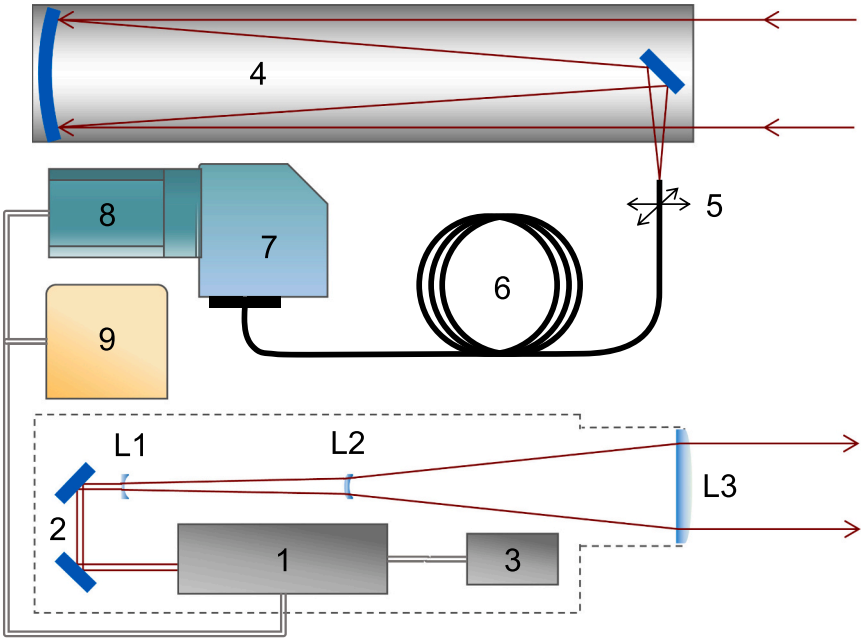

Fig. 2. Schematic of the C2 instrument illustrating the emitter (dashed line) and receiver modules: 1) laser head, 2) folding mirrors, 3) batteries, L1-L3 focusing beam expander as per Tables 3, 4) receiver unit, 5) fibre optic incoupling, 6) fibre optic cable, 7) spectrograph, 8) iCCD detector, 9) computer.

Table 3
Components and performance of the two optical designs prepared for the emitter module of configuration C2. Glass is BK7 in both designs.

Configuration	Focal length/diameter (mm/mm)			Expansion ratio	Length (mm)	Airy disk diameter (μm)		Diffraction encircled energy (%)	
	L_1	L_2	L_3			25 m	50 m/70 m	25 m	50 m/70 m
OD1	−75/25	−150/25.4	500/125	10×	677	410	840/1180	96.7	96.4/96.7
OD2	−30/12.7	−100/25.4	200/75	8×	290	520	1030	96.4	96.6/–

Table 4
Characteristics of the two spectrometers used.

Option	Spectrograph						Detector			Total weight (Kg)	
	Focal length (mm)	Slit (um)	Grating (l/mm)	Blaze (nm)	Bandpass (nm)	Resolution (nm)	Technology	Active matrix (w x h)	Data transfer	w/o PC	w/ PC
S1	75	25	1800 static	250	220	0.25	CMOS	4096 × 1	USB	0.18	0.28
S2	163	25	1200 manual	300	86	0.26	18-mm intesifier + CCD	1330 × 512	PCI card	6,5	12

the telescope output to the slit [30]. A round-to-linear fibre optic bundle was ordered but not delivered in time for travel either.

A dual-sided commercial tripod mount oriented to astrophotographers was used to hold together the laser emitter and the receiver telescope. This mount has two standard dovetail clamps which allow quick repetitive mounting of the sub-units and provides the ability to aim the instrument at the target. In addition, a push-pull screw set in the dovetails provides some degree of parallax adjustment.

2.3. Deployment at the volcano

Indeed, the need for parallax correction is a weakness of the modular configuration as it is required for setting the distance to the sample. Moreover, because it was not well implemented mechanically, it consumed precious time at the field. The whole process involved several steps: (i) firstly, the laser emitter was focussed by rotation of the L_3 tube mount to a setting where the shockwaves were clearly audible on top of the volcano noise, (ii) then a red diode laser was sent through the fibre optic cable and the telescope to the lava sample and was overlapped with the plasma using the adjusting screws in the dovetail. Even though this procedure had worked well during the indoor tests of the instrument, once in the field, the adjustment was found to lack the necessary precision. Thus, a further fine-tuning adjustment was put together using a spare *x-y* mount which was added to the existing *z*-adjustment at the coupling between the telescope output and the tip of the fibre. (iii) at the final step of the procedure, the laser focus setting was further optimized using the spectrometer reading.

Once the modules of the instrument were mounted and aligned, operation was simple since the double-sided tripod mount provided jaw and pitch aiming for the whole instrument and the signal depth-of-focus tolerance for the emitter/collector was ±1 m at a 40 m range not including the additional resources to fine focussing the laser emitter by rotating the L_3 lens tube mount, and the light collector with the *x-y-z* mount.

Support with the laser operation, range measuring and thermal imaging was provided by personnel of the Spanish Military Emergency Unit (UME) who supported the whole operation at the exclusion zone, including transport, power supply for the iCCD detector, monitorization of exposure to noxious gases or guidance in our way through the lava streams sidestepping high-temperature patches and vents which reached up to 390 °C. Conditions were extreme for both the people and the instrument the two times at the exclusion zone. At over 750 m above the Atlantic Ocean, the weather was windy, alternating rapidly between sunny and cloudy, the latter occasionally accompanied by light rain. Wind gusts carried fine ash particles that ended up entering the computer and the detector despite being fitted with filtering elements. The telescope tube and the L_3 lens of the emitter were obviously the most exposed elements but no apparent performance degradation or damage was noticed during or after the tests. The personal protection equipment consisted of a helmet, an FFP3 mask, laser and dust safety goggles, a high-visibility vest, heat-resistant footwear and a full face-covering gas mask used for safe evacuation of the exclusion area when gas alarms are

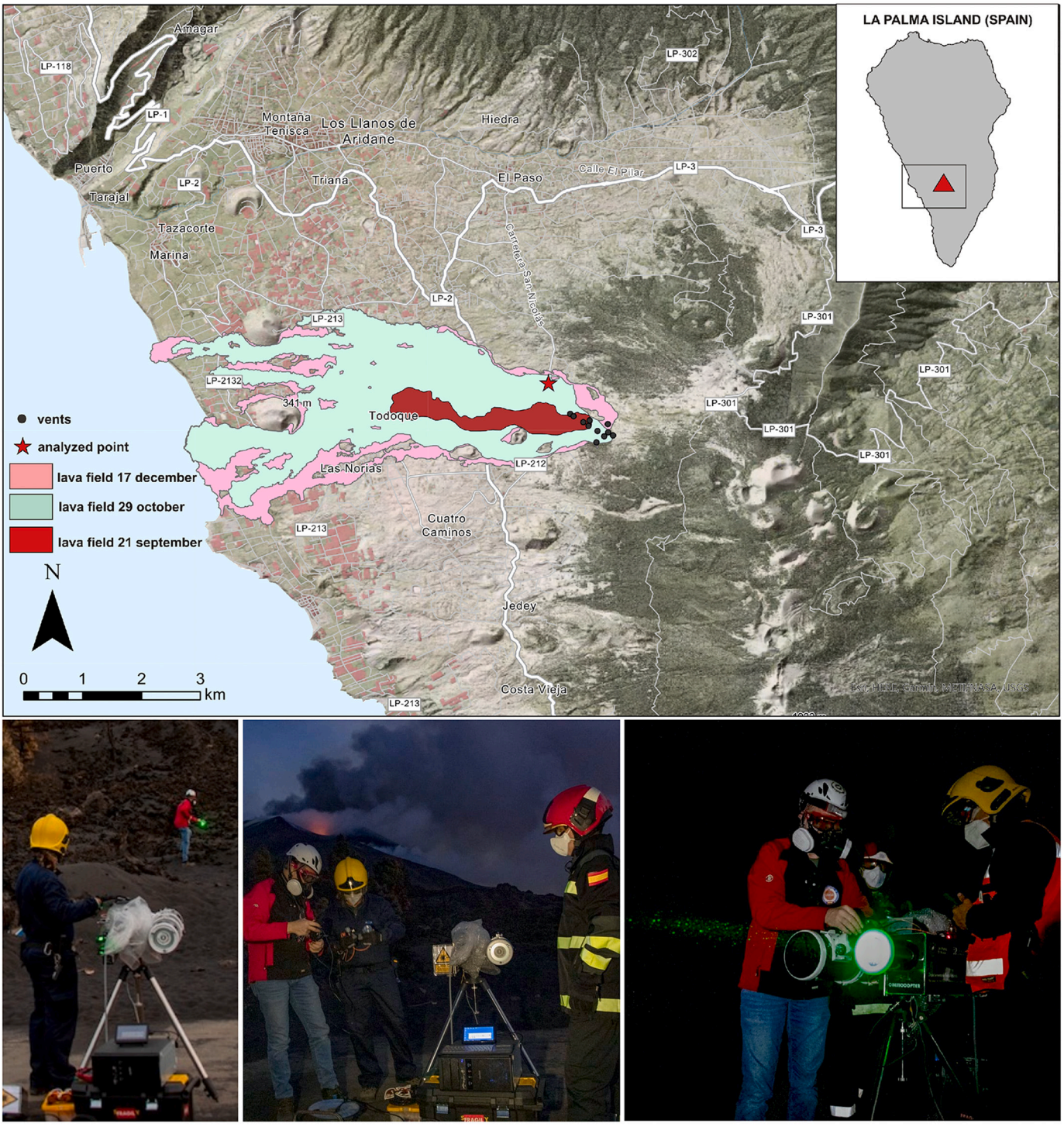

Fig. 3. Top: map of the La Palma Island showing the lava fields, (●) the location of the Cumbre Vieja volcano vents and (★) the sampling point (28°37′19.6″N 17°52′25.7″W). Bottom: snapshots of the instrument at the field featuring FL (UME), IGJ, RPL and SP during the instrument setup on November 5th, 2021.

triggered (filter labelled ABEK P3 + Hg, 2.5 μm particles, organic vapour inorganic and acid gas filters plus ammonia and mercury vapour).

Understandably, time at the exclusion zone was limited and out of the four days at La Palma, only two sessions of measurements could be held. The system was fully disassembled for transport and reassembled at the Advanced Command Post (PMA) the first day. The first session at the field lasted two hours and mainly consisted in optimizing the optical alignment and acquiring the first spectra at 40 from a solidified lava stream located at 28°37′18.5"N 17°52′25.7"W -the exact position of the instrument was chosen to be 40 m in the normal direction from the lava wall and on a flat surface remaining from the LP-212 road. The geographical location of the measurements and several snapshots of the instrument during the measurements are shown in Fig. 3. The fourth day (November 7th, 2021) the second session took place. It lasted five hours

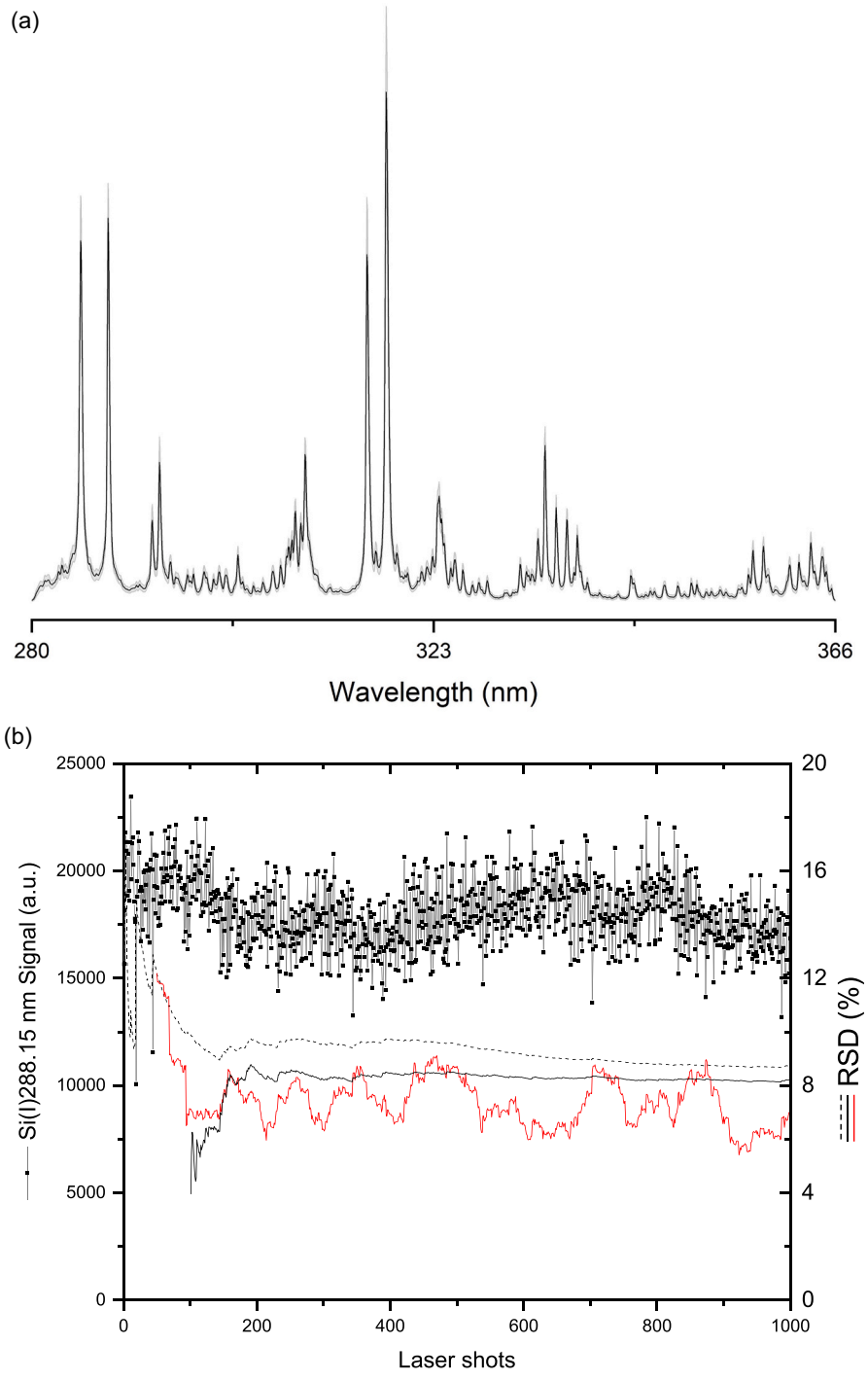

Fig. 4. (a) Average LIBS spectrum from a series of 1000 individual spectra of sample LP212–02 acquired under calm wind conditions showing the signal variability as a two-standard-deviation band. (b and d) On the left axis, evolution of the Si(I) 288.15 nm signal for the two series of 1000 spectra in (a) and (c) and (right axis) evolution of the relative standard deviation (RSD) calculated as (dashed line) a cumulative set of spectra starting at the first laser shot, (black solid line) a cumulative set of spectra starting at laser shot #101, (red solid line) a moving boxcar of 50 spectra. (c) Average LIBS spectrum from a series of 1000 individual spectra acquired under gusty wind conditions showing the signal variability as a two-standard-deviation band. (For interpretation of the references to colour in this figure legend, the reader is referred to the web version of this article.)

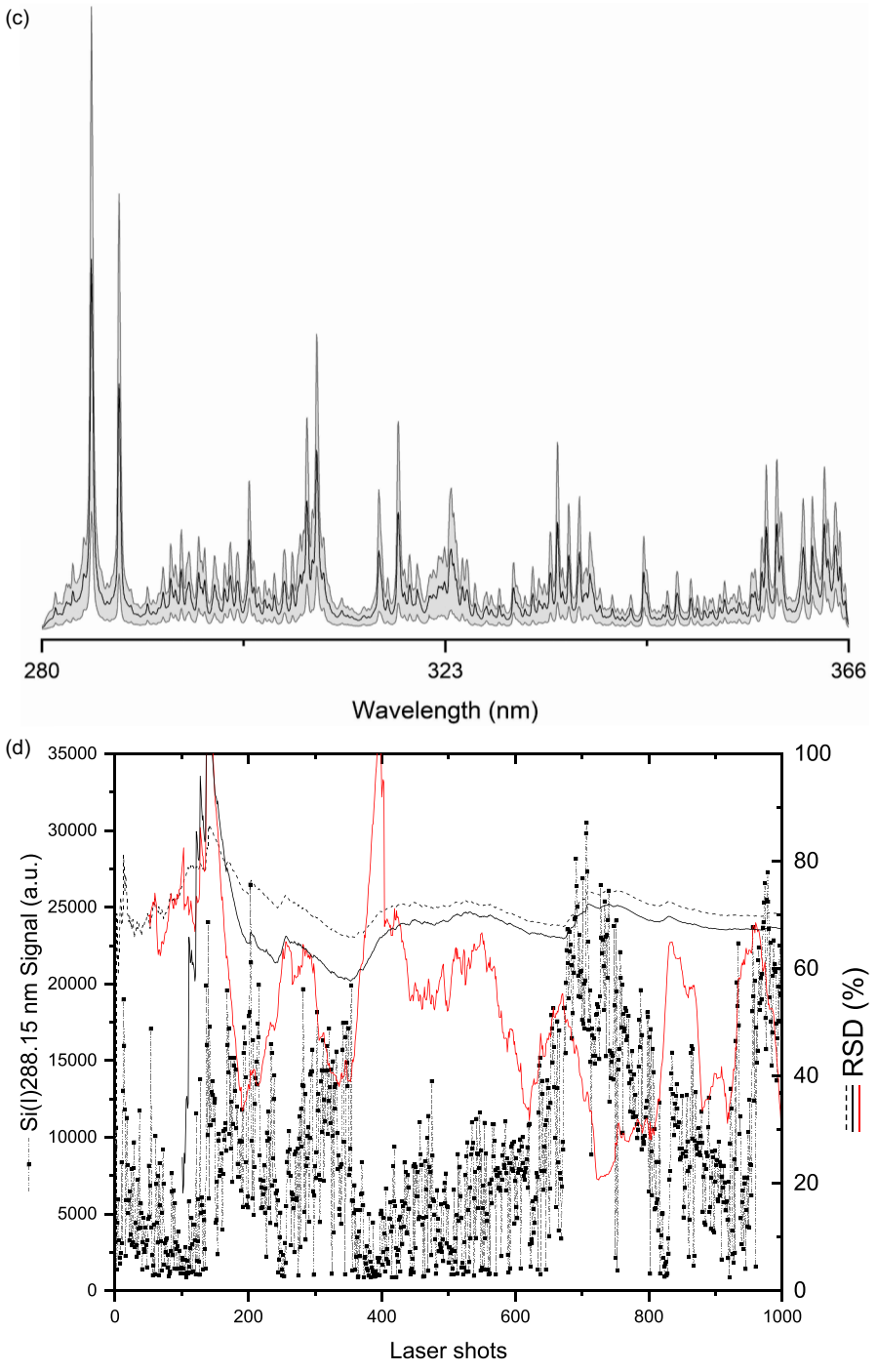

Fig. 4. (*continued*).

and was plagued with strong wind gusts, intermittent rain, power cuts and finally, a gas alarm (HCl + rain), which put an end to the session and to the field tests.

3. Results and discussion

3.1. Preliminary results

Pending to collect a full set of lava samples for calibration once the eruption concludes and all the streams are safe enough to be walked and sampled, some preliminary results and conclusions are presented here. Fig. 4-a presents a lava spectrum (Sample LP212–02, 17:14 UTC) obtained by averaging a series of 1000 spectra acquired under low-wind conditions (1.9 ms^{-1}) at 40 m. Two standard deviations around the average spectrum are contained in the shadowed area. The plot shows an excellent signal-to-noise ratio in these conditions. The only reason to acquire 1000 spectra was recording sufficient data for statistics and study the long-term behavior of the ablation process with the battery-powered laser source. Firing 1000 shots demands both battery performance and good heat management of the passively cooled laser unit. As Fig. 4-b illustrates, after a clean out period of 150 laser shots, which dusts off the ash and any possibly remaining moisture -the lava stream temperature was 85–117 °C- the signal for the Si(I) line at 288.158 nm is stable enough to obtain a relative standard deviation (RSD) with an

average of 50 spectra, which is similar to that for the 1000 spectra average. No significant improvements were found when averaging more than 50 spectra, but the step-like shapes in the boxcar plot are indicative that even light wind can induce instrument fluctuations which affect the stand-off pointing stability and the measurements [12].

As soon as the wind picked up (up to 13.1 ms^{-1}), the variability of the signal increased as revealed by the spectrum in Fig. 4-c and the Si(I) 288.158 nm signal plots in Fig, 4-d. Lava heterogeneity and surface unevenness are the main reasons for such variability, and although the laser incidence was always normal to the lava wall, the surface roughness of the sample affects the incidence angle of the laser beam, and in turn, the fraction of the pulse energy coupled for the plasma ignition [31].

It must be noted that, even though the lava spectra in Figs. 5 and 6 were obtained by firing 1000 laser shots in the absence of wind gusts, there was a residual fluctuation as illustrated by Fig 4-b. Therefore, the average spectrum compiles information from an irregular sample volume which is about 4 mm in diameter due to the wandering of the sub-millimeter laser beam and the series of individual spectra is not valid for depth profiling purposes. Fig. 5 shows the average spectrum of the sample in Fig. 4 (LP212–02) along with the spectra of several metallic and salt samples used for identification purposes. The emission of Si, Mg, Al, Ca, Mn, Ti and Fe could be identified and the main spectral lines assigned. These spectral signatures are in good agreement with the composition as measured by x-ray fluorescence spectroscopy (Table 5) of the samples once it was safe. However, the feature-rich emission of Fe and Ti makes it very difficult to isolate non-interfered lines for other minor elements like Mn, Cr or the remaining transition elements, present in the tens and hundreds of ppm. As expected, the resolution of the setup is not sufficient to deal with the quantitative analysis with solvency, at least, in this spectral window, but it showed great potential for semi-quantitative approaches.

As an example, Fig. 6 compares the spectra of samples LP212–02 and LP212–07. The latter is a lava sample located about five meters away from the former in the same lava stream (40.3 m from the instrument, 17:23 UTC) that presented a reddish hue to the naked eye. It was measured under the same wind conditions as LP212–02. Both spectra have been normalized to the Ti emission, which is approximately invariant in most samples, and then overlapped to reveal the subtle differences, mainly consisting in a slightly higher Fe contribution in sample LP212–07 and the presence of Mn, Cu and Na (Fig. S1 contains a deconvolution of the Mn(I) 353.212 emission line for samples LP212–02 and LP212–07). There is also a noticeably lower Ca(II) contribution in the spectrum of LP212–07 which could lead to think of a lower content in this element. Still, the higher Mg(I)/Mg(II) ratio in LP212–07 suggests that a lower plasma temperature, might be the reason for the lower Ca (II) signal, rather than or in addition to a difference in the Ca content. This is in good agreement with the quantitative analysis in Table 5.

3.2. Principal component analysis

Even if its exact composition is not known, the type of lava flowing

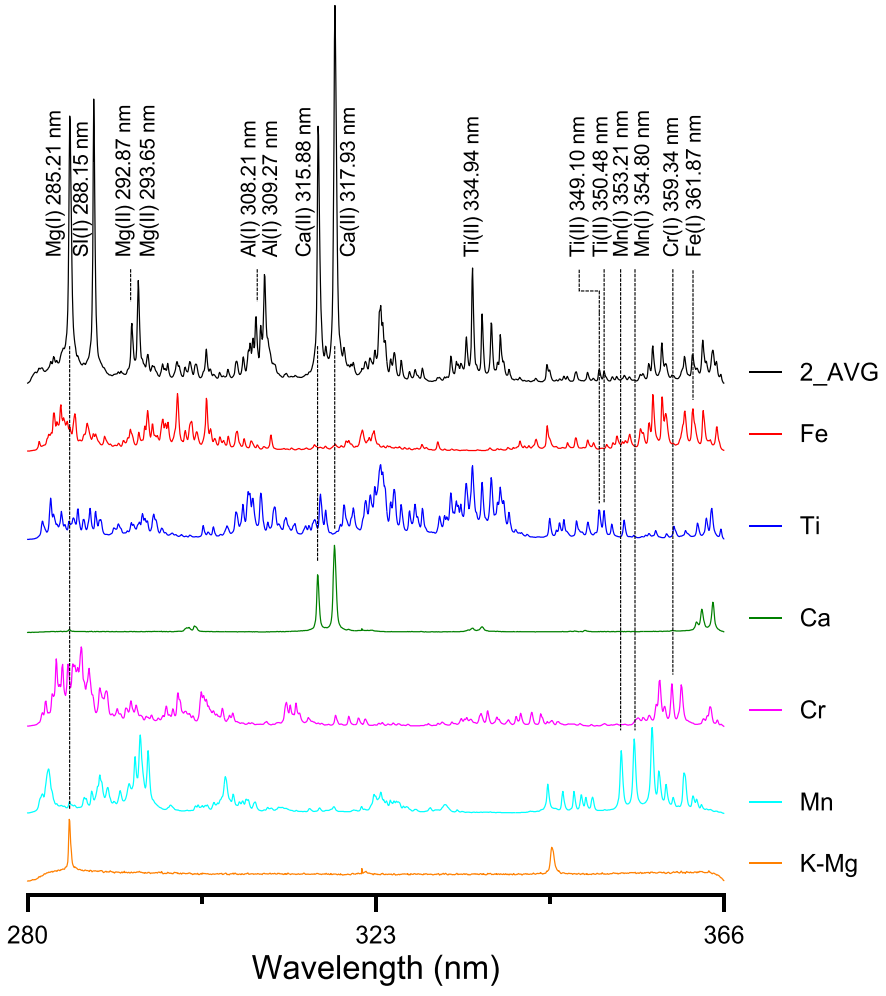

Fig. 5. (a) Average (1000 shots) LIBS spectra of sample LP212–02 and of several metallic and salt samples (average of 300 shots). The latter were acquired at the PMA at a 22 m distance. The intensity scale has been changed for comparison purposes.

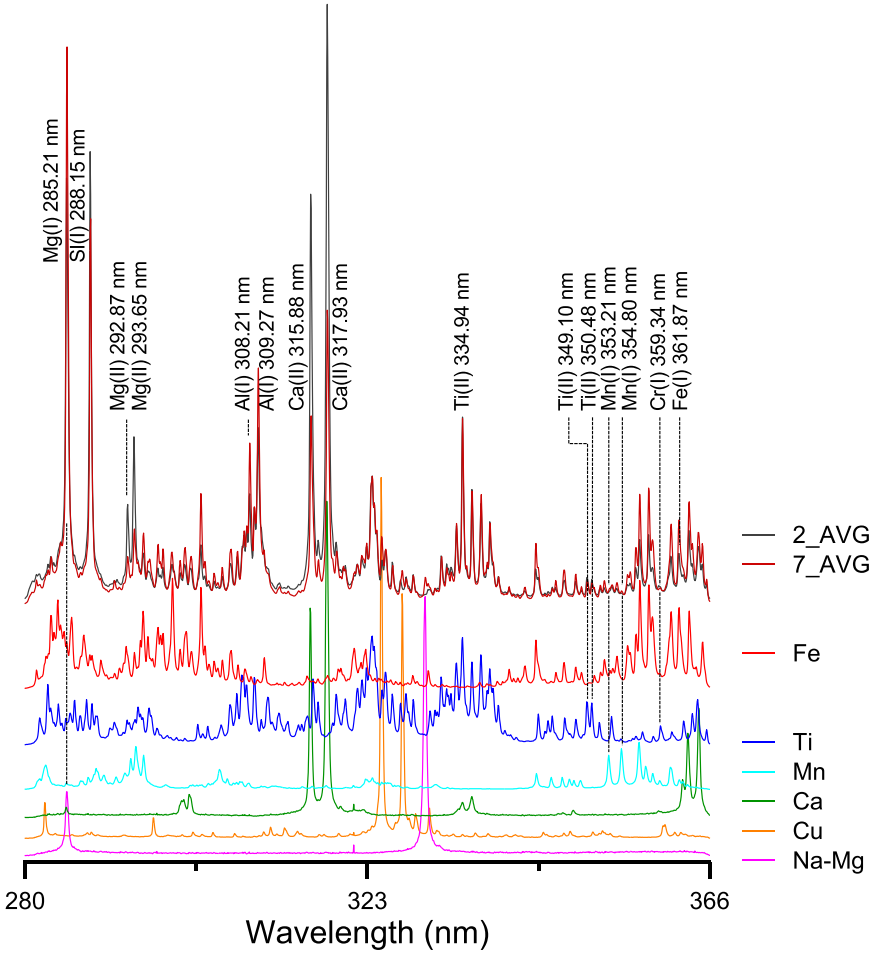

Fig. 6. (a) Average LIBS spectrum of sample LP212–02 (as in Fig. 5) compared to the spectra of sample LP212–07, obtained with the same acquisition and averaging parameters. Both spectra have been normalized to match the Ti emission. Spectra of the metallic and salt samples are an average of 300 shots and were acquired at the PMA at a 22 m distance.

Table 5
Compositions of samples LP212–01, LP212–02 and LP212–07 as measured with XRF.

Element	Concentration (% w/w)		
	LP212–01	LP212–02	LP212–07
Si	20.75	13.69	16.91
Fe	9.19	10.32	11.04
Ca	8.21	6.48	7.34
Al	6.69	5.12	6.66
Mg	5.33	1.99	2.62
Ti	1.98	1.93	2.04
K	1.13	0.94	1.03
Mn	0.15	0.13	0.25
Sr	0.09	0.11	0.11
	Concentration (ppm)		
Ba	–	749	989
Cu	114	186	234
V	379	496	400
Zr	330	350	349
Cr	366	267	342
Sb	–	192	104

on a stream is a telltale about its source depth, and thus, about the stage of the eruption. Principal component analysis (PCA) is a well-known technique which can reduce the volume of data and the complexity of spectral interpretation and yet deliver valuable information to a geologist, provided that the spectral window and resolution used gathers sufficient information. Thus, 1000 spectra for each of samples were used in the PCA. Samples LP212–02, LP212–07, LP212,01 (17:05 UTC, distance 40.1 m same location as LP212–02 but a different grey shade), and LP212–06 (17:20 UTC, distance 40.3 m, same location as LP212–07 and similar reddish hue) were analyzed under the same calm wind conditions. It was found that 91.6% of the variance is contained in the first four PC and the analysis of the loadings and the biplot revealed that most of the variance which can lead to sample discrimination is associated with Mg, Si, Al Ca and Fe (PC2 and PC4) but not with Ti (PC3). This is in good agreement with that found during the manual analysis of the spectra and the elemental content of the samples in Table 5. The scores for PC4 are plotted vs those for PC2 in Fig. 7-a which shows a good discrimination capacity for three types of samples while matching samples LP212–06 and LP212–07. The latter makes sense as both series of spectra were acquired from positions in the stream approximately 5 cm away from each other.

It is worth noting that this is not a surface residue analysis where the number of laser pulses that one can fire at the sample is limited by the amount of sample available. Therefore, firing a high number of pulses (1000 shots for each sample in Fig. 7-a) is affordable, the degree of confidence of the result understandably being much higher. Consequently, it may be tempting to process each data series as a depth profile into the sample but it must be considered that the beam wandering on the surface prevents to do so as the shot number is not a monotonous function of depth into the sample surface [12]. Nevertheless, some depth-related information can be extracted by comparing different

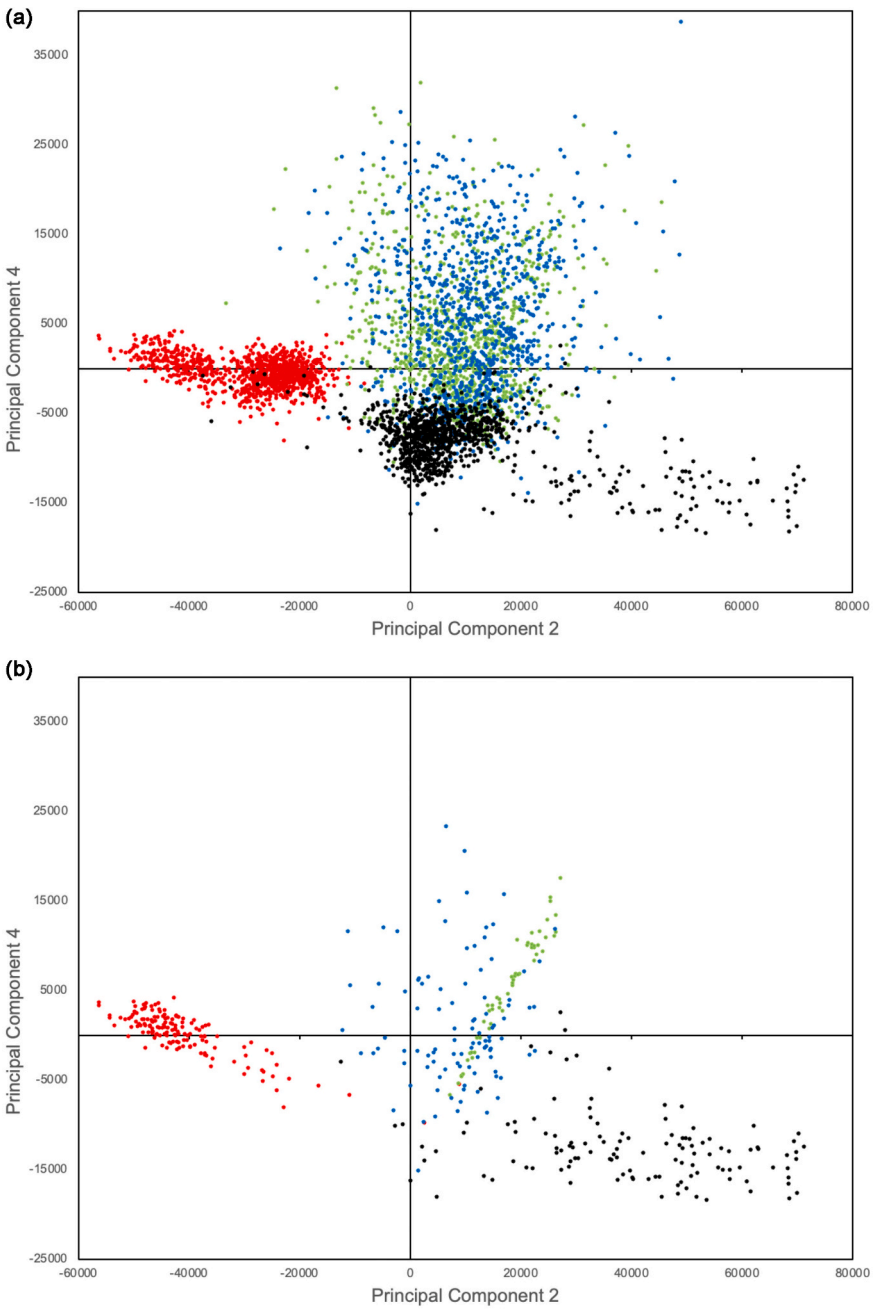

Fig. 7. Scores plots of the principal component analysis carried out on 4000 spectra corresponding to samples (●) LP212–01, (■) LP212–02, (◆) LP212–06 and (▲) LP212–07 [32]. 1000 spectra have been analyzed for each sample. (a) Plot of the 1000 points of each of the four series. (b) Plot of the first 120, 150, 55 and 100 points of the series, respectively. (c) Plot of the last 500 points of each of the series. Past 4 software has been used for PCA [32].

subsets of spectra with a certain distance within each series. In Fig 7-b a subset of the first points of each series in Fig 7-a has been plotted (see figure caption for further detail on the shot numbers). The first 50–150 shots in each series hit the fresh sample surface which is partially covered with a thin layer of fine ash powder and material which has been in contact with the atmospheric oxygen while at high temperature. As shown in Fig. 7-b, such spectra corresponding to the sample surface tend to appear in tails or plumes appended to the main cluster for their respective samples. Although these initial spectra would be representative of the ash covering the sample and should cluster together, a possible explanation for the behavior observed is that the ash powder is fine enough to let a significant portion of the beam reach the sample surface. This is supported by the results in Fig 7-c where the last 500 points of the four series are plotted, showing the main bodies of the clusters separately from those in Fig. 7-b.

4. Conclusions

A portable instrument was designed and built from scratch in a short time period of three weeks. The modular design made possible its transport by one person in a regular commercial flight and then assemble it prior to its first use at a lava stream. The performance of the laser and the emitter optics was par to that expected from the design, but parallax adjustment proved a weakness of the instrument, mostly due to mechanical issues. This consumed valuable time at the field but once fixed, light collection to the intensified spectrometer produced spectra

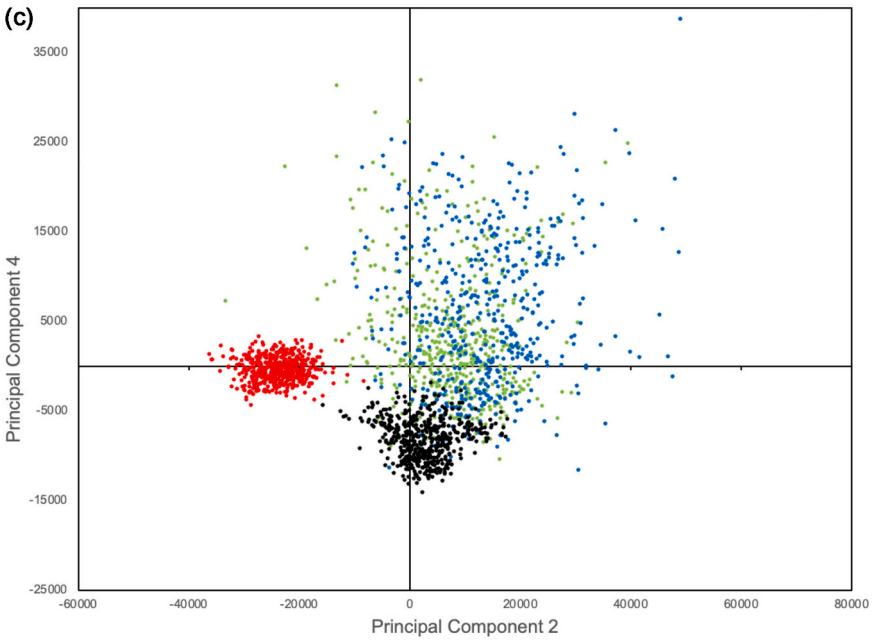

Fig. 7. (*continued*).

with excellent signal-to-noise ratio. Although the spectrometer did not provide sufficient spectral resolution and the window was not wide enough to register all the elements of interest, the data acquired contained enough information for a semiquantitative approach. The results obtained demonstrate that, in spite of the subtle spectral differences among the samples and the signal variability induced by the wind, there was sufficient information and a statistical approach to data processing such as PCA could extract this information and be used as a classification tool. At the time of writing these lines, the eruption has been declared as finished by the Spanish authorities. Future work will be directed to elaborate a chemical map of all the lava streams using the Chemocopter airborne LIBS instrument.

Declaration of Competing Interest

The authors declare that they have no known competing financial interests or personal relationships that could have appeared to influence the work reported in this paper.

Acknowledgements

We express our sincere gratitude to the Spanish Unidad Militar de Emergencias (UME) for providing essential support, security, and expertise at the field. We would like to thank Carlos Malagón (Astroshop, Málaga, Spain) for donating the telescope used in the stand-off LIBS instrument, to the personnel of the Chemical Analysis Area and the Machine Shop of the Central Facility for Research Support (SCAI-UMA) and to Profs. E.R. Losilla and A. Cabeza (Dept. Química Inorgánica, Cristalografía y Mineralogía, UMA) and D. Marrero (Dept. Física Aplicada I, UMA) for their valuable comments and advice with the surrogate samples. This work has been partially supported by the I Plan Propio de Investigación de la Universidad de Málaga, the Extraordinary Funding (RD 1078/2021, 7th December, Núm. 293 Sec. I. Pág. 150,995) and PID2020-113407RB-I00 granted by the Spanish Ministry of Science and Innovation (MICINN).

Appendix A. Supplementary data

Supplementary data to this article can be found online at https://doi.org/10.1016/j.sab.2022.106391.

References

[1] L. Becerril, I. Galindo, A. Gudmundsson, J.M. Morales, Depth of origin of magma in eruptions, Sci. Rep. 3 (2013) 2762, https://doi.org/10.1038/srep02762.
[2] J. Martí, A. Castro, C. Rodríguez, F. Costa, S. Carrasquilla, R. Pedreira, X. Bolos, Correlation of magma evolution and geophysical monitoring during the 2011–2012 El Hierro (Canary Islands) submarine eruption, J. Petrol. 54 (2013) 1349–1373, https://doi.org/10.1093/petrology/egt014.
[3] G.S. Michelfelder, T.C. Feeley, A.D. Wilder, The volcanic evolution of Cerro Uturuncu: a high-K, composite volcano in the back-arc of the Central Andes of SW Bolivia, Int. J. Geosci. 5 (2014) 1263–1281, https://doi.org/10.4236/ijg.2014.511105.
[4] M.W. Loewen, H.R. Dietterich, N. Graham, P. Izbekov, Evolution in eruptive style of the 2018 eruption of Veniaminof volcano, Alaska, reflected in groundmass textures and remote sensing, Bull. Volcanol. 83 (2021) 72, https://doi.org/10.1007/s00445-021-01489-6.
[5] A. Hernandez-Pacheco, M.C. Valls, The historic eruptions of La Palma Island (canaries), Arquipélago. Série Ciências Da Natureza. 3 (1982) 83–94.
[6] A. Klügel, K. Galipp, K. Hoernle, F. Hauff, S. Groom, Geochemical and volcanological evolution of La Palma, Canary Islands, J. Petrol. 58 (2017) 1227–1248, https://doi.org/10.1093/petrology/egx052.
[7] B. Sallé, P. Mauchien, S. Maurice, Laser-induced breakdown spectroscopy in open-path configuration for the analysis of distant objects, Spectrochim. Acta B At. Spectrosc. 62 (2007) 739–768, https://doi.org/10.1016/j.sab.2007.07.001.
[8] W. Li, X. Li, X. Li, Z. Hao, Y. Lu, X. Zeng, A review of remote laser-induced breakdown spectroscopy, Appl. Spectrosc. Rev. 55 (2020) 1–25, https://doi.org/10.1080/05704928.2018.1472102.
[9] D.A. Cremers, R.C. Wiens, M.J. Ferris, J.D. Blacic, Development and testing of a prototype LIBS instrument for a NASA Mars rover, in: A. Sawchuk (Ed.), Laser Induced Plasma Spectroscopy and Applications, Optical Society of America, Orlando, Florida, 2002, p. ThE22, https://doi.org/10.1364/LIBS.2002.ThE22.
[10] R.C. Wiens, S. Maurice, B. Barraclough, M. Saccoccio, W.C. Barkley, J.F. Bell, S. Bender, J. Bernardin, D. Blaney, J. Blank, M. Bouyé, N. Bridges, N. Bultman, P. Caïs, R.C. Clanton, B. Clark, S. Clegg, A. Cousin, D. Cremers, A. Cros, L. DeFlores, D. Delapp, R. Dingler, C. D'Uston, M. Darby Dyar, T. Elliott, D. Enemark, C. Fabre, M. Flores, O. Forni, O. Gasnault, T. Hale, C. Hays, K. Herkenhoff, E. Kan, L. Kirkland, D. Kouach, D. Landis, Y. Langevin, N. Lanza, F. LaRocca, J. Lasue, J. Latino, D. Limonadi, C. Lindensmith, C. Little, N. Mangold, G. Manhes, P. Mauchien, C. McKay, E. Miller, J. Mooney, R.V. Morris, L. Morrison, T. Nelson, H. Newsom, A. Ollila, M. Ott, L. Pares, R. Perez, F. Poitrasson, C. Provost, J. W. Reiter, T. Roberts, F. Romero, V. Sautter, S. Salazar, J.J. Simmonds, R. Stiglich, S. Storms, N. Striebig, J.-J. Thocaven, T. Trujillo, M. Ulibarri, D. Vaniman, N. Warner, R. Waterbury, R. Whitaker, J. Witt, B. Wong-Swanson, The ChemCam instrument suite on the Mars science laboratory (MSL) rover: body unit and combined system tests, Space Sci. Rev. 170 (2012) 167–227, https://doi.org/10.1007/s11214-012-9902-4.
[11] R.C. Wiens, S. Maurice, S.H. Robinson, A.E. Nelson, P. Cais, P. Bernardi, R. T. Newell, S. Clegg, S.K. Sharma, S. Storms, J. Deming, D. Beckman, A.M. Ollila, O. Gasnault, R.B. Anderson, Y. André, S. Michael Angel, G. Arana, E. Auden, P. Beck, J. Becker, K. Benzerara, S. Bernard, O. Beyssac, L. Borges, B. Bousquet, K. Boyd, M. Caffrey, J. Carlson, K. Castro, J. Celis, B. Chide, K. Clark, E. Cloutis, E. C. Cordoba, A. Cousin, M. Dale, L. Deflores, D. Delapp, M. Deleuze, M. Dirmyer,

C. Donny, G. Dromart, M. George Duran, M. Egan, J. Ervin, C. Fabre, A. Fau, W. Fischer, O. Forni, T. Fouchet, R. Fresquez, J. Frydenvang, D. Gasway, I. Gontijo, J. Grotzinger, X. Jacob, S. Jacquinod, J.R. Johnson, R.A. Klisiewicz, J. Lake, N. Lanza, J. Laserna, J. Lasue, S. Le Mouélic, C. Legett, R. Leveille, E. Lewin, G. Lopez-Reyes, R. Lorenz, E. Lorigny, S.P. Love, B. Lucero, J.M. Madariaga, M. Madsen, S. Madsen, N. Mangold, J.A. Manrique, J.P. Martinez, J. Martinez-Frias, K.P. McCabe, T.H. McConnochie, J.M. McGlown, S.M. McLennan, N. Melikechi, P.-Y. Meslin, J.M. Michel, D. Mimoun, A. Misra, G. Montagnac, F. Montmessin, V. Mousset, N. Murdoch, H. Newsom, L.A. Ott, Z.R. Ousnamer, L. Pares, Y. Parot, R. Pawluczyk, C. Glen Peterson, P. Pilleri, P. Pinet, G. Pont, F. Poulet, C. Provost, B. Quertier, H. Quinn, W. Rapin, J.-M. Reess, A.H. Regan, A. L. Reyes-Newell, P.J. Romano, C. Royer, F. Rull, B. Sandoval, J.H. Sarrao, V. Sautter, M.J. Schoppers, S. Schröder, D. Seitz, T. Shepherd, P. Sobron, B. Dubois, V. Sridhar, M.J. Toplis, I. Torre-Fdez, I.A. Trettel, M. Underwood, A. Valdez, J. Valdez, D. Venhaus, P. Willis, The SuperCam instrument suite on the NASA Mars 2020 Rover: body unit and combined system tests, Space Sci. Rev. 217 (2020) 4, https://doi.org/10.1007/s11214-020-00777-5.

[12] S. Palanco, S. Aranda, F. Mancebo, M.C. López-Escalante, D. Leinen, J.R. Ramos-Barrado, Towards airborne laser-induced breakdown spectroscopy: a signal recovery method for LIBS instruments subjected to vibrations, Spectrochim. Acta B At. Spectrosc. 187 (2022) 106342, https://doi.org/10.1016/j.sab.2021.106342.

[13] Chemocopter. https://www.chemocopter.com/, 2022 (accessed August 11, 2021).

[14] T. Seel, S. Ruppin, Eliminating the Effect of Magnetic Disturbances on the Inclination Estimates of Inertial Sensors, IFAC-PapersOnLine 50, 2017, pp. 8798–8803, https://doi.org/10.1016/j.ifacol.2017.08.1534.

[15] C. Lopez-Moreno, S. Palanco, J.J. Laserna, F. DeLucia, A.W. Miziolek, J. Rose, R. A. Walters, A.I. Whitehouse, Test of a stand-off laser-induced breakdown spectroscopy sensor for the detection of explosive residues on solid surfaces, J. Anal. At. Spectrom. 21 (2006) 55–60, https://doi.org/10.1039/b508055j.

[16] B. Sallé, D. Cremers, S. Maurice, R. Wiens, P. Fichet, Evaluation of a compact spectrograph for in-situ and stand-off laser-induced breakdown spectroscopy analyses of geological samples on Mars missions, Spectrochim. Acta B At. Spectrosc. 60 (2005) 805–815, https://doi.org/10.1016/j.sab.2005.05.007.

[17] R.S. Harmon, F.C. DeLucia, C.E. McManus, N.J. McMillan, T.F. Jenkins, M. E. Walsh, A. Miziolek, Laser-induced breakdown spectroscopy – an emerging chemical sensor technology for real-time field-portable, geochemical, mineralogical, and environmental applications, Appl. Geochem. 21 (2006) 730–747, https://doi.org/10.1016/j.apgeochem.2006.02.003.

[18] R. Gaudiuso, M. Dell'Aglio, O.D. Pascale, G.S. Senesi, A.D. Giacomo, Laser induced breakdown spectroscopy for elemental analysis in environmental, cultural heritage and space applications: a review of methods and results, Sensors 10 (2010) 7434–7468, https://doi.org/10.3390/s100807434.

[19] G. Nicolodelli, J. Cabral, C.R. Menegatti, B. Marangoni, G.S. Senesi, Recent advances and future trends in LIBS applications to agricultural materials and their food derivatives: An overview of developments in the last decade (2010–2019). Part I. Soils and fertilizers, TrAC Trends Anal. Chem. 115 (2019) 70–82, https://doi.org/10.1016/j.trac.2019.03.032.

[20] W. Hao, X. Hao, Y. Yang, X. Liu, Y. Liu, P. Sun, R. Sun, Rapid classification of soils from different mining areas by laser-induced breakdown spectroscopy (LIBS) coupled with a PCA-based convolutional neural network, J. Anal. At. Spectrom. 36 (2021) 2509–2518, https://doi.org/10.1039/D1JA00078K.

[21] R.S. Harmon, G.S. Senesi, Laser-induced breakdown spectroscopy – a geochemical tool for the 21st century, Appl. Geochem. 128 (2021) 104929, https://doi.org/10.1016/j.apgeochem.2021.104929.

[22] V. Geovanna, C.V. Cesar, Semi quantitative Elemental Analysis of Volcanic Ashes from Populations Surrounding the Tungurahua Volcano of the Eruptive Period 2008–2010, Using the LIBS Spectroscopy (Laser-Induced Breakdown Spectroscopy), in: Latin America Optics and Photonics Conference (2018), Paper Tu4A.26, Optical Society of America, 2018, p. Tu4A.26, https://doi.org/10.1364/LAOP.2018.Tu4A.26.

[23] E. Teran-Hinojosa, H. Sobral, I. Hernández-Mendoza, C. Márquez-Herrera, G. González-Hernández, Laser-induced breakdown spectroscopy characterization of tree rings from the Popocatépetl volcano area, Mexico, Spectrochim. Acta B At. Spectrosc. 161 (2019) 105713, https://doi.org/10.1016/j.sab.2019.105713.

[24] D.M. Bower, C.S.C. Yang, T. Hewagama, C.A. Nixon, S. Aslam, P.L. Whelley, J. L. Eigenbrode, F. Jin, J. Ruliffson, J.R. Kolasinski, A.C. Samuels, Spectroscopic characterization of samples from different environments in a Volcano-Glacial region in Iceland: implications for in situ planetary exploration, Spectrochim. Acta A Mol. Biomol. Spectrosc. 263 (2021) 120205, https://doi.org/10.1016/j.saa.2021.120205.

[25] S. Palanco, L.M. Cabalin, D. Romero, J.J. Laserna, Infrared laser ablation and atomic emission spectrometry of stainless steel at high temperatures, J. Anal. At. Spectrom. 14 (1999) 1883–1887, https://doi.org/10.1039/a905472c.

[26] C. Lopez-Moreno, S. Palanco, J.J. Laserna, Quantitative analysis of samples at high temperature with remote laser-induced breakdown spectrometry using a room-temperature calibration plot, Spectrochim. Acta Part B-Atom. Spectr. 60 (2005) 1034–1039, https://doi.org/10.1016/j.sab.2005.05.037.

[27] C. Lopez-Moreno, S. Palanco, J.J. Laserna, Calibration transfer method for the quantitative analysis of high-temperature materials with stand-off laser-induced breakdown spectroscopy, J. Anal. At. Spectrom. 20 (2005) 1275–1279, https://doi.org/10.1039/b508528d.

[28] S. Palanco, S. Conesa, J.J. Laserna, Analytical control of liquid steel in an induction melting furnace using a remote laser induced plasma spectrometer, J. Anal. At. Spectrom. 19 (2004) 462–467, https://doi.org/10.1039/b400354c.

[29] J.C. Carracedo, E.R. Badiola, H. Guillou, J. de la Nuez, F.J.P. Torrado, Geology and volcanology of La Palma and El Hierro, Western Canaries, Estud. Geol. 57 (2001) 175–273, https://doi.org/10.3989/egeol.01575-6134.

[30] S. Palanco, J. Laserna, Remote sensing instrument for solid samples based on open-path atomic emission spectrometry, Rev. Sci. Instrum. 75 (2004) 2068–2074, https://doi.org/10.1063/1.1753675.

[31] S. Palanco, J.M. Baena, J.J. Laserna, Open-path laser-induced plasma spectrometry for remote analytical measurements on solid surfaces, Spectrochim. Acta Part B-Atom. Spectr. 57 (2002) 591–599, https://doi.org/10.1016/s0584-8547(01)00388-3.

[32] Ø. Hammer, D.A.T. Harper, P.D. Ryan, Past: paleontological statistics software package for education and data analysis, Palaeontol. Electron. 4 (2001), 9pp.